

Pulmonary Vascular Resistance and Impedance in Isolated Mouse Lungs: Effects of Pulmonary Emboli

HOLLY A. TUCHSCHERER, EIDAN B. WEBSTER, and NAOMI C. CHESLER

Department of Biomedical Engineering, University of Wisconsin, Madison, WI 53706-1609

(Received 25 August 2004; accepted 24 October 2005)

Abstract—To study pulsatile pressure-flow rate relationships in the intact pulmonary vascular network of mice, we developed a protocol for measuring pulmonary vascular resistance and impedance in isolated, ventilated, and perfused mouse lungs. We used pulmonary emboli to validate the effect of vascular obstruction on resistance and impedance. Main pulmonary artery and left atrial pressures and pulmonary vascular flow rate were measured under steady and pulsatile conditions in the lungs of C57BL/6J mice ($n = 6$) before and after two infusions with 25 μ m-diameter microspheres (one million per infusion). After the first and second embolizations, pulmonary artery pressures increased approximately two-fold and three and a half-fold, respectively, compared to baseline, at a steady flow rate of 1 ml/min ($P < 0.05$). Pulmonary vascular resistance and 0 Hz impedance also increased after the first and second embolizations for all flow rates tested ($P < 0.05$). Frequency-dependent features of the pulmonary vascular impedance spectrum were suggestive of shifts in the major pulmonary vascular reflection sites with embolization. Our results demonstrate that pulmonary artery pressure, resistance, and impedance magnitude measured in this isolated lung setup changed in ways consistent with *in vivo* studies in larger animals and humans and demonstrate the usefulness of the isolated, ventilated, and perfused mouse lung for investigating steady and pulsatile pressure-flow rate relationships.

Keywords—Microspheres, Pulmonary embolism, Impedance spectrum, Right ventricular hydraulic afterload, Murine.

INTRODUCTION

In pulmonary hypertension, the pressure and flow characteristics of the pulmonary vascular system deviate from the normal state. Pulmonary vascular resistance and pulmonary vascular impedance are two of the parameters typically calculated to estimate the severity of pulmonary hypertension, and to predict the increased work and stress on the heart.^{15,20,21} In particular, resistance and impedance have been measured in animal models such as rats, dogs, goats, and pigs.^{8,11,18,22,32} To our knowledge, the effects

of pulmonary hypertension on pulsatile pressure-flow rate relationships in mice have not been investigated.

Isolated, ventilated, and perfused mouse lungs have been used to investigate pulmonary vascular reactivity and steady pressure-flow rate relationships in response to acute hypoxia^{9,12,34} and in the presence of genetic defects.^{1,10,17,27} Mice are an especially advantageous animal model for pulmonary research because knockout and transgenic mice, which are becoming more widely available, are valuable in studying the molecular mechanisms of pulmonary diseases. However, the small size of the mouse can make the task of obtaining quality *in vivo* data challenging. To date, only steady flow perfusion has been used in the isolated, ventilated, and perfused mouse lung, which limits the information about pressure-flow rate relationships that can be derived from these studies. To investigate frequency-dependent responses to pulmonary disease such as pulmonary hypertension, pulsatile flow at physiological frequencies must be used.

In this study, we created pulsatile pulmonary vascular flow, which is the analog of right ventricular output in a whole animal, with mechanical pumps that could produce a wide range of both steady and sinusoidal flow rates at physiological frequencies in a technique pioneered by Caro and McDonald.⁴ Consequently, we could measure the pulmonary vascular pressure-flow rate relationships for a range of flow magnitudes and pulsation frequencies in the isolated, ventilated, and perfused mouse lung. We measured these pressure-flow rate relationships before and after two rounds of pulmonary embolization with microspheres in order to validate the ability of the setup to quantify increases in resistance and impedance due to obstruction. In particular, based on the literature on *in vivo* studies in larger animals, we sought to demonstrate that emboli would increase pulmonary vascular resistance (PVR), increase impedance magnitude at 0 Hz (Z_0) and cause changes in high frequency impedance. We also investigated changes in the characteristic impedance Z_C , index of wave reflection R_w and frequency of the first minimum in the impedance magnitude (f_{min}).

Address correspondence to Naomi C. Chesler, Department of Biomedical Engineering, University of Wisconsin-Madison, 2146 Engineering Centers Building, 1550 Engineering Drive, Madison WI 53706-1609. Electronic mail: chesler@engr.wisc.edu

82 **METHODS AND MATERIALS**

83 *Animal Handling*

84 Three female and three male 10–12 week old C57BL/6J
 85 mice, 24 ± 5 g weight were used (Jackson Laboratory,
 86 Bar Harbor, ME). Mice were anesthetized with an in-
 87 traperitoneal injection of 150 mg/kg pentobarbital solution.
 88 All protocols and procedures were approved by the Uni-
 89 versity of Wisconsin Institutional Animal Care and Use
 90 Committee.

91 *Isolated Lung Preparation*

92 After confirmation of deep anesthesia, the animal was
 93 placed in a chamber for isolated lung ventilation and
 94 perfusion (IL-1 system, Hugo Sachs Elektronik, March-
 95 Hugstetten, Germany). The chamber was heated to 37°C to
 96 maintain body temperature. A tracheotomy was performed,
 97 and a stainless steel ventilation cannula was inserted into
 98 the tracheal stoma. The distal trachea was secured to the
 99 cannula with suture. Thereafter, the animal was ventilated
 100 with room air at 90 breaths/min with peak inspiratory and
 101 expiratory pressures of 10 and 2 cm H_2O , respectively,
 102 and an inspiratory/expiratory ratio of 1:1, as previously
 103 reported.³¹ Airway pressure and airway flow rate were
 104 measured with pressure and flow transducers (MPX and
 105 Validyne 45–14, respectively, Hugo Sachs Elektronik).
 106 Deep breaths to 20 cm H_2O every 10 min were performed
 107 to prevent atelectasis.³¹

108 Then, a thoracotomy was performed and 500 U/100 g
 109 body weight heparin was injected into the right ventricle
 110 to prevent blood clotting. The animal was euthanized by
 111 exsanguination, and the lower abdomen removed. Once
 112 identified and isolated, the pulmonary artery was cannulated
 113 through an incision in the right ventricle and secured in
 114 place by a suture around the pulmonary artery. The left
 115 atrium was subsequently cannulated through an incision in
 116 the left ventricle. The left atrial cannula was positioned and
 117 held in place by the mitral valve ring without suture.

118 Thus instrumented, the lung vasculature was perfused
 119 with 3.5% Ficoll (Sigma-Aldrich, St. Louis, MO) in RPMI
 120 1640 cell culture medium (Cellgro, Mediatech, Inc., Herndon,
 121 VA) preheated to 37°C . Steady flow was driven by a
 122 syringe pump (Cole Palmer Instrument Company, Vernon
 123 Hills, IL) and passed through a heat exchanger (at 37°C) and
 124 bubble trap before reaching the pulmonary artery. Pulsatile
 125 flow was driven by a high frequency oscillatory piston pump
 126 (EnduraTEC Systems Corporation, Minnetonka, MN) op-
 127 erated in parallel with the syringe pump. Flow exited the
 128 left atrium into approximately 20 cm of small diameter tub-
 129 ing (ID = 1.03 mm), which then exited to the atmosphere
 130 at the same elevation as the left atrial cannula. Thus, left
 131 atrial pressure was equal to the sum of atmospheric pres-
 132 sure and the viscous pressure drop in the tubing, which was
 133 linearly proportional to the flow rate. The lungs and heart

were routinely wetted with 1% phosphate buffered saline 134
 solution (PBS) spray. The lungs were kept on positive- 135
 pressure ventilation throughout the experiment. Pulmonary 136
 artery pressure (P_{PA}) and left atrial pressure (P_{LA}) were 137
 measured by pressure transducers (P75, Hugo Sachs Elek- 138
 tronik) connected to the pulmonary artery and left atrium 139
 cannulas by approximately 20 cm of small diameter (ID = 140
 0.77 mm), nearly rigid tubing. Pulmonary vascular flow rate 141
 (Q) was measured by an in-line flowmeter (Transonic Sys- 142
 tems, Inc., Ithaca, NY) placed approximately 6 cm upstream 143
 from the pulmonary artery cannula. All pressures and flows 144
 were monitored by continuous display (LabView 6.1, Na- 145
 tional Instruments, Austin, TX) on a laptop computer (Dell 146
 Latitude, Round Rock, TX). See Fig. 1 for schematic of the 147
 isolated, ventilated, and perfused lung setup. 148

149 *Initial Measurements*

To obtain initial steady flow rate measurements of P_{PA} , 150
 P_{LA} , and Q , the lungs were perfused at 1 ml/min until 151
 pressure stabilized, approximately 4–5 min. This perfusion 152
 rate was determined by previously reported flow rates for 153
 isolated perfused mouse lungs.³¹ Data were recorded for 5 s 154
 at 15 Hz, while keeping lungs inflated at the end-inspiratory 155
 pressure of 10 cm H_2O . Lungs were kept inflated to the end- 156
 inspiratory pressure during data collection to prevent edema 157
 and to normalize the effects of airway pressure and volume 158
 on P_{PA} , P_{LA} , and Q .²⁰ 159

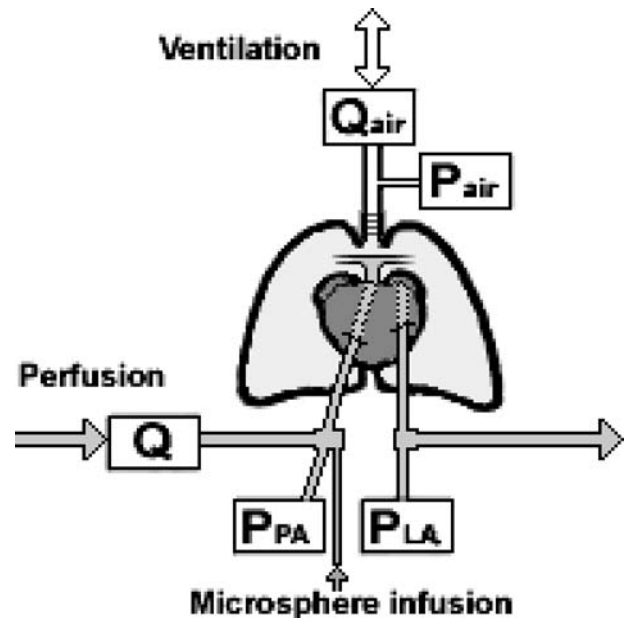


FIGURE 1. Isolated, ventilated, and perfused mouse lung setup showing cannulas and relative transducer locations for pulmonary artery pressure P_{PA} , left atrial pressure P_{LA} , perfusate flow rate Q , airway pressure P_{air} , and airway flow rate Q_{air} .

160	<i>Pulsatile Flow Rate Measurements</i>	
161	The steady flow rate was gradually increased to	210
162	3 ml/min, and sinusoidal flow rates of the form $Q = 3 +$	211
163	$2 \sin(2\pi f t)$ ml/min were generated for frequencies $f =$	212
164	1,2,5,10,15, and 20 Hz for a total of 22 s. This frequency	213
165	range was chosen to include the physiological heart rate	214
166	for mice (~ 10 Hz). P_{PA} , P_{LA} , and Q were recorded at	215
167	200 Hz. Similar to the initial steady flow rate measure-	216
168	ments, lungs were kept inflated at end-inspiratory pressure	217
169	(10 cm H ₂ O) during data collection. After the sinusoidal	218
170	flow rate measurements were performed, the steady flow	219
171	rate was gradually reduced to 0.5 ml/min and normal ven-	220
172	tilation of 90 breaths/min resumed. The pulsatile flow rate	221
173	measurements were repeated multiple times. Between re-	
174	peated measurements, there was 1 min of steady flow at	
175	0.5 ml/min with a ventilation rate of 90 breaths/min.	
176	<i>Steady Flow Rate Measurements</i>	
177	After the last pulsatile flow rate measurement, at least	
178	1 min of steady flow at 0.5 ml/min was imposed, and then	
179	the flow rate was increased to 1 ml/min. The steady flow	
180	rate was then increased from 1 ml/min to 5 ml/min in	
181	1 ml/min steps at 10 s. intervals while P_{PA} , P_{LA} , and Q were	
182	recorded at 15 Hz. Lungs were inflated to end-inspiratory	
183	pressure during data collection as before. The steady flow	
184	rate was then reduced to 1 ml/min, and normal ventilation	
185	of 90 breaths/min resumed.	
186	<i>Addition of Microspheres</i>	
187	After the initial, pulsatile, and steady flow rate mea-	
188	surements, which constitute the baseline conditions for	
189	a given mouse lung, microspheres were infused into the	
190	pulmonary vasculature to simulate pulmonary embolism.	
191	Perfusion was set at 0.5 ml/min and ventilation was	
192	90 breaths/min during the infusion. Approximately $1 \times$	
193	10^6 25 μ m polystyrene microspheres (crosslinked with di-	
194	vinylbenzene) with a coefficient of variance of 20% (Poly-	
195	sciences, Inc, Warrington, PA) were combined with 5 ml	
196	heated perfusion media (3.5% Ficoll in RPMI). The micro-	
197	sphere mixture was added at approximately 1 ml/min by	
198	syringe through a portal in the pulmonary artery cannula	
199	(see Fig. 1). Microspheres were sonicated before infusion	
200	to prevent clumping; however, some may have aggregated	
201	into clusters of 2 or 3 during the infusion. The initial, pul-	
202	satile, and steady flow rate measurements described above	
203	then were repeated to obtain the first embolization values.	
204	After these data were collected, another 1×10^6 micro-	
205	spheres were infused by the same method, and the second	
206	embolization values were acquired.	
207	<i>Lung Fixation and Histology</i>	
208	After all data were collected, the ventilation and per-	
209	fusion were stopped and the lungs were removed from the	
	isolated lung system. The lungs were fixed with paraformal-	210
	dehyde (3% in PBS) infused through the trachea; lungs were	211
	not inflated during infusion. Freezing compound OCT was	212
	then perfused through the trachea, and the entire lung was	213
	snap frozen in 2-methyl butane cooled by liquid nitrogen.	214
	Four sections with a thickness of 7 μ m were cut from each	215
	lung at -20°C on a cryostat. The sections were stained with	216
	hematoxylin to indicate vascular and airway cell nuclei.	217
	Sections were imaged on an inverted microscope (TE-2000,	218
	Nikon, Melville, NY) and captured using a spot camera and	219
	software for image digitization (MetaVue, Optical Analysis	220
	Systems, Nashua NH).	221
	<i>Calculations</i>	222
	The pressure drop across the pulmonary vascular net-	223
	work (ΔP) was calculated as the pulmonary artery pressure	224
	minus the left atrial pressure ($P_{PA} - P_{LA}$). Under steady	225
	flow conditions, flow rate and pressures were averaged over	226
	50 data points to obtain P_{PA} , ΔP , and Q for a given flow	227
	rate magnitude. Pulmonary vascular resistance (PVR) was	228
	calculated as $\Delta P/Q$.	229
	Under pulsatile flow conditions, data obtained during	230
	one full sinusoidal cycle were analyzed at each frequency.	231
	Calculated parameters included impedance, characteristic	232
	impedance, input impedance, and index of wave reflection.	233
	The impedance was calculated in the frequency domain	234
	using fast Fourier transforms. ²⁰ Specifically, the magnitude	235
	of the impedance (Z) was calculated as the ratio of the	236
	ΔP modulus to the Q modulus ²⁴ using MATLAB (Math-	237
	Works, Inc., Natick, MA). The zeroth and first harmonic	238
	values were found for each imposed sinusoidal flow rate	239
	frequency. The phase angle between ΔP and Q waves for	240
	one cycle at each frequency, indexed to the time at which	241
	$Q = 3$ ml/min, was also analyzed using MATLAB. Charac-	242
	teristic impedance (Z_C) was calculated as the average of the	243
	impedance magnitudes between the first minimum (5 Hz at	244
	baseline) and 20 Hz. ¹⁹ The same 5–20 Hz range was used	245
	to calculate Z_C after the first and second embolizations. The	246
	average impedance at the zeroth harmonic ($f = 0$ Hz) for	247
	all frequencies was taken as the input resistance (Z_0). The	248
	index of wave reflection (R_w) was calculated using $R_w =$	249
	$(Z_0 - Z_C)/(Z_0 + Z_C)$. ²⁰	250
	<i>Statistics</i>	251
	Data were analyzed using a paired-Wilcoxon signed rank	252
	test. P -values less than 0.05 were considered significant.	253
	No differences were observed between male and female	254
	mice so all data were grouped. Statistical analyses were	255
	performed using SAS statistical software (SAS Institute	256
	Inc., Cary, NC). All data are presented in terms of mean	257
	value \pm standard deviation.	258

259

RESULTS

260

Initial Measurements

261 At baseline conditions, the initial measurement of P_{PA}
 262 was 11 ± 1 mmHg at 1 ml/min flow rate (Fig. 2). In response
 263 to the first and second infusions of microsphere emboli, P_{PA}
 264 increased significantly ($P < 0.05$ compared to baseline for
 265 both). Under all conditions, the pressures measured initially
 266 were higher than those measured with steady perfusion but
 267 after pulsatile flow (see Fig. 3 at 1 ml/min).

268

Steady Flow Rate Measurements

269 Under all conditions, P_{PA} increased as flow rate in-
 270 creased from 1 to 5 ml/min (Fig. 3). The dependence of
 271 P_{PA} on flow rate was well described by a power law func-
 272 tion (as suggested by²⁸) at baseline and after the first and
 273 second embolizations ($R^2 > 0.98$ for all conditions). In
 274 all cases, P_{LA} increased approximately linearly due to the
 275 Poiseuille-type losses in the outflow tubing. After both the
 276 first and second embolizations, P_{PA} values were higher than
 277 baseline for all flow rates tested ($P < 0.05$). Compared to
 278 the first embolization, P_{PA} and the change in P_{PA} with a
 279 change in Q were greater after the second embolization,
 280 but the differences were not significant.

281 PVR was 7.7 ± 0.6 mmHg ml⁻¹ min at 1 ml/min under
 282 baseline conditions and decreased as flow rate increased
 283 from 1 to 5 ml/min ($P < 0.05$ between all flow rates)
 284 (Fig. 4). After both the first and second embolizations, PVR
 285 also decreased with increasing flow rate ($P < 0.05$). After
 286 both the first and second embolizations, PVR values were
 287 higher than baseline for all flow rates tested ($P < 0.05$).
 288 There were increases in the average PVR at all flow rates
 289 between the first and second embolizations, but they were
 290 not significant.

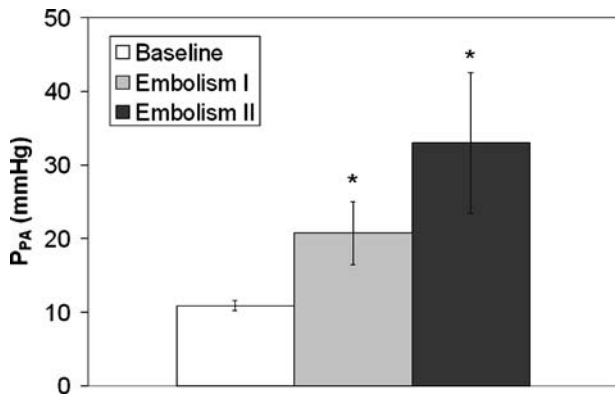


FIGURE 2. Initial measurements of pulmonary artery pressure P_{PA} for steady perfusion at baseline and after the first and second embolizations at 1 ml/min. Bars represent mean \pm standard deviation ($n = 6$). * $P < 0.05$ vs. baseline.

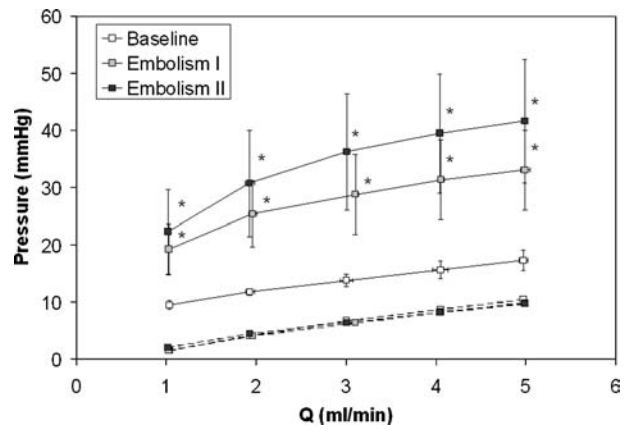


FIGURE 3. Pulmonary artery pressure P_{PA} (solid lines) and left atrial pressure P_{LA} (dashed lines) versus flow rate (Q) for steady perfusion at baseline and after the first and second embolizations. Bars represent mean \pm standard deviation ($n = 6$). * $P < 0.05$ vs. baseline.

Pulsatile Flow Rate Measurements

291

292 Under baseline conditions, average 0 Hz impedance
 293 magnitude, or input resistance (Z_0) was $2.1 \pm$
 294 0.4 mmHg ml⁻¹ min and increased significantly after both
 295 the first and second embolizations ($P < 0.05$, Fig. 5).
 296 Impedance magnitudes at frequencies above 0 Hz were
 297 much lower than those at 0 Hz and were significantly differ-
 298 ent after embolization at high frequencies. The impedance
 299 phase was significantly more negative after embolization up
 300 to 10 Hz ($P < 0.05$); there were no differences at 15–20 Hz
 301 (Fig. 5).

302 The impedance magnitude data above 0 Hz were re-
 303 plotted to highlight the differences at nonzero frequencies
 304 (Fig. 6). At low frequencies (1–5 Hz), impedance mag-
 305 nitude (Z) showed little variation as a function of frequency at
 306

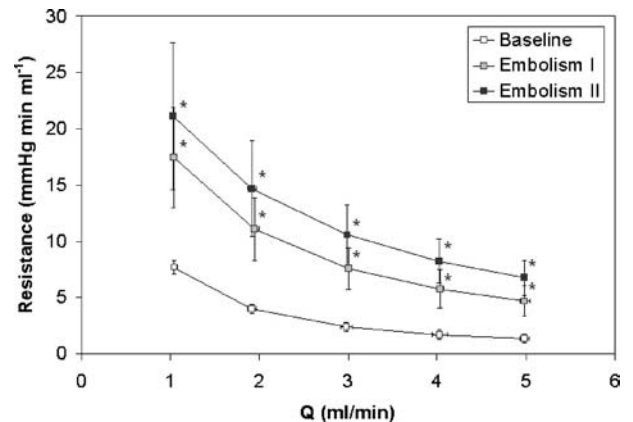


FIGURE 4. Pulmonary vascular resistance versus flow rate for steady perfusion at baseline and after the first and second embolizations. Bars represent mean \pm standard deviation ($n = 6$). * $P < 0.05$ vs. baseline.

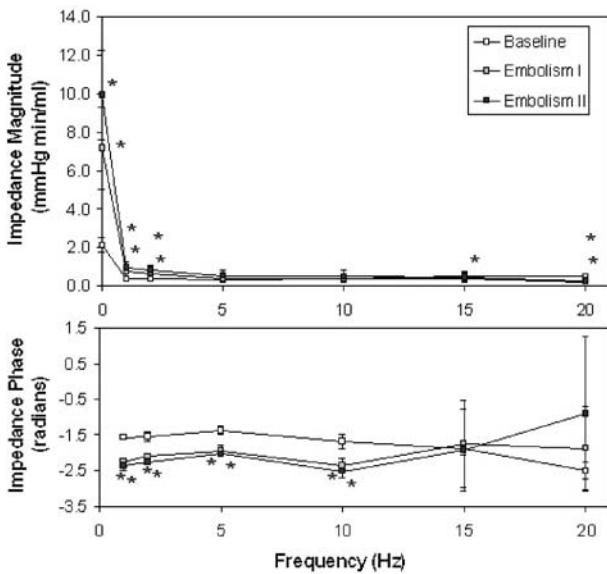


FIGURE 5. Pulmonary vascular impedance magnitude and phase versus frequency at baseline and after the first and second embolizations. The pulmonary vascular perfusate flow was $Q = 3 + 2 \sin(2\pi f t)$ ml/min for $f = 1, 2, 5, 10, 15,$ and 20 Hz, and data were recorded at the end-inspiratory pressure of 10 cm H_2O . Bars represent mean \pm standard deviation ($n = 6$). * $P < 0.05$ vs. baseline.

306 baseline. As frequency increased, Z also increased; values
 307 at 10 – 20 Hz were slightly but significantly larger than the
 308 5 Hz value ($P < 0.05$). The first minimum of impedance
 309 magnitude (f_{\min}) was at 5 Hz. After both the first and sec-
 310 ond embolizations, Z was high at low frequencies and low
 311 at high frequencies. In particular, Z values at low frequen-
 312 cies (1 – 2 Hz) were significantly higher than values at high
 313 frequencies (10 – 20 Hz) ($P < 0.05$); f_{\min} was equal to or

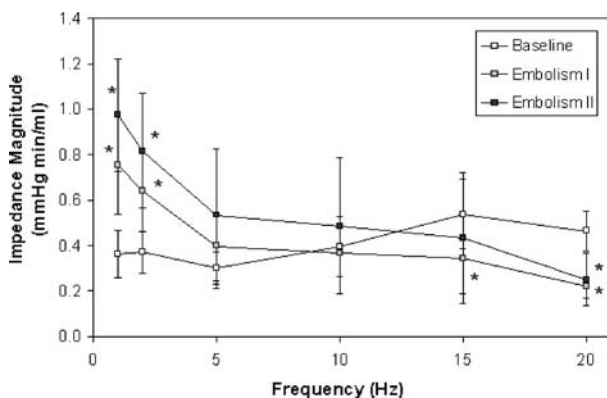


FIGURE 6. Pulmonary vascular impedance magnitude for frequencies above 0 Hz at baseline and after the first and second embolizations. The pulmonary vascular perfusate flow was $Q = 3 + 2 \sin(2\pi f t)$ ml/min for $f = 1, 2, 5, 10, 15,$ and 20 Hz, and data were recorded at the end-inspiratory pressure of 10 cm H_2O . Bars represent mean \pm standard deviation ($n = 6$). * $P < 0.05$ vs. baseline.

greater than 20 Hz. Also, at low frequencies (1 – 2 Hz), Z after both embolizations were higher than at baseline ($P < 0.05$) whereas at high frequencies (15 – 20 Hz), the reverse was true. Also, the impedance magnitudes after the second embolization were higher than those after the first embolizations at all frequencies.

Characteristic impedance (Z_C) was 0.43 ± 0.10 mmHg ml^{-1} min at baseline and decreased slightly to 0.31 ± 0.11 and 0.39 ± 0.22 mmHg ml^{-1} min after the first and second embolization, but these differences were not significant. Average wave reflection index (R_w) was 0.66 ± 0.06 at baseline and increased significantly to 0.92 ± 0.02 and 0.92 ± 0.03 after the first and second embolizations, respectively ($P < 0.05$).

Histology

To ensure that microspheres reached both lungs in all experiments, hemotoxylin-stained sections were examined for each lung. All sections from right and left lungs showed microspheres in pulmonary vessels and not in alveolar spaces (Fig. 7), which would have been evidence of tissue damage during OCT perfusion or repositioning of spheres during sectioning and staining. Perfusion and ventilation appeared to cause minimal edema or damage to lung tissue.

DISCUSSION

Pulmonary artery and left atrial pressures in response to steady and pulsatile flows were measured before and after two infusions of $25 \mu m$ microspheres in isolated, ventilated, and perfused mouse lungs. Microsphere infusion increased P_{PA} , PVR, pulmonary vascular impedance at 0 Hz, and low frequencies, and shifted f_{\min} to higher frequencies. Our results demonstrate that steady and pulsatile pressure-flow rate relationships can be measured in isolated, ventilated, and perfused mouse lungs, and that embolic pulmonary hypertension has similar effects in mice as in larger animals.

Initial Measurements

At baseline, pulmonary artery pressure measured before pulsatile perfusion was approximately 11 mmHg at a flow rate of 1 ml/min; recent studies in isolated, ventilated, and perfused mouse lungs have shown similar baseline pressures despite differences in perfusate and mouse strain.^{1,10,27} With microsphere embolization, P_{PA} increased significantly. An increase in P_{PA} with microsphere embolism previously has been measured in larger animal models including rats, dogs, goats, and pigs.^{3,6,11,22,26,29,32} Also, on average, the initial P_{PA} was higher than that measured at the same flow rate after pulsatile perfusion. This finding suggests that preconditioning with pulsatile perfusion decreases resistance and should be performed prior to data collection in isolated lung experiments.

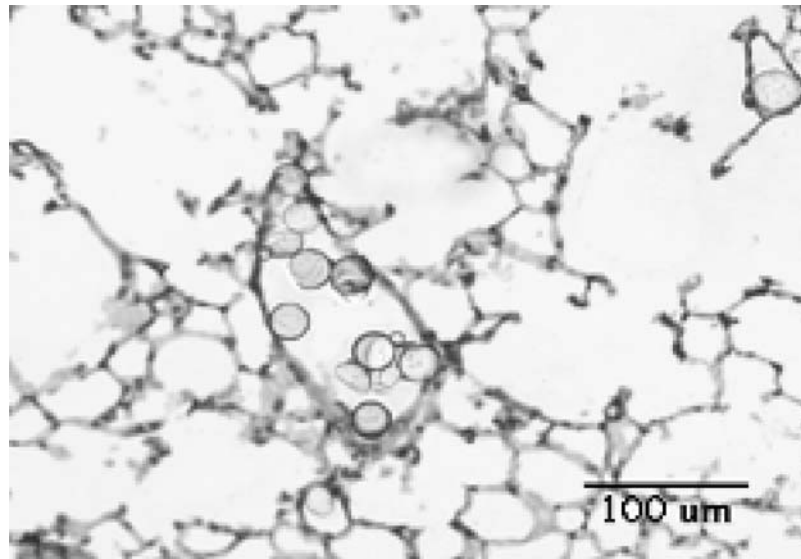


FIGURE 7. Representative histological section (hematoxylin stained) of lung parenchyma showing microspheres in large and small pulmonary arteries. Scale bar is 100 μm .

363 *Steady Pressure-Flow Rate Relationships*

364 At baseline conditions, the difference between P_{PA} and
 365 P_{LA} , or ΔP was nearly constant as flow rate increased from
 366 1 to 5 ml/min. By contrast, Parker *et al.* found that ΔP in-
 367 creased slightly for increasing flow rates in isolated mouse
 368 lungs, but only investigated between 0.3 and 1.0 ml/min.²⁷
 369 At higher flow rates, such as those used in our study, capil-
 370 lary recruitment, distention, and a shift in lung zones (from
 371 1 at low flows to 3 at high flows) may account for the con-
 372 stancy of ΔP with increasing flow.³⁰ After embolization,
 373 ΔP increased with increasing flow rates, suggesting that
 374 the recruitment of capillaries and distension of microves-
 375 sels could not compensate completely for the obstruction
 376 caused by emboli in the lungs. Hence, larger pressure drops
 377 across the pulmonary vascular network were generated,
 378 which increased with increasing flow rate.

379 For all conditions, PVR decreased with increasing flow
 380 rate. The PVR after both embolizations were higher than
 381 at baseline for all flow rates examined. This last finding is
 382 consistent with previous research in larger animal models
 383 in which the lungs were embolized with 15 μm micro-
 384 spheres,¹¹ 100 μm glass beads,^{5,6,26} 0.5 mm glass beads,³²
 385 and autologous blood clot ($<1 \text{ cm}^3$).¹³ While each infusion
 386 of 1×10^6 25 μm microspheres increased PVR, the changes
 387 from the first embolization to the second (as a function of
 388 flow rate) were not statistically significant. Glenny *et al.*
 389 found a linear relationship between the number of 15 μm -
 390 diameter microspheres infused into isolated rat lungs and
 391 the increase in pulmonary vascular resistance.¹¹ An im-
 392 portant scaling factor is likely the ratio of infused solid
 393 volume to circulating lung blood volume. While the equiv-
 394 alent solid volumes infused were similar (a maximum of

8.8 mm^3 in [11] vs. 8.2 and 1.64 mm^3 , after embolism I 395
 and II, respectively), the rat circulating blood volume is 396
 clearly larger. Thus, taken together, these studies suggest 397
 that at low ratios of solid to lung blood volume, resistance 398
 increases linearly with solid volume infused but that at high 399
 ratios the relationship is sublinear. 400

Pulsatile Pressure-Flow Rate Relationships 401

At baseline, the change in impedance as a function of 402
 frequency was as follows: the highest impedance value oc- 403
 curred at 0 Hz (Z_0), followed by a minimum at 5 Hz, and 404
 a local maximum at 15 Hz. The existence of a maximum 405
 at 0 Hz followed by a minimum and fluctuations at higher 406
 frequencies is the classic pulmonary vascular impedance 407
 pattern, and is consistent with many other studies in an- 408
 imals and humans.^{8,16,18,20,26,30,32} After embolization, Z_0 409
 increased significantly compared to baseline. This increase 410
 represents the increased opposition to mean flow through 411
 the pulmonary vascular system due to the microsphere em- 412
 boli. Under pulsatile flow conditions, with a mean flow 413
 rate of 3 ml/min, Z_0 at baseline and after embolization 414
 were comparable to PVR at the same flow rate and condi- 415
 tion. Therefore, the overall resistive response of the lungs 416
 was similar whether steady or pulsatile flow was used. An 417
 increase in Z_0 with microsphere, glass bead, and autol- 418
 ogous blood clot embolization previously has been mea- 419
 sured in larger animal models including dogs, goats, and 420
 pigs.^{3,18,22,26,32} 421

The characteristic impedance Z_C did not vary signifi- 422
 cantly after embolization, but did show a slight decreasing 423
 trend. Changes in Z_C after pulmonary embolization have 424
 been shown to differ with species. For example, Z_C in dog 425

426 lungs decreased after pulmonary embolization with 0.5 mm
 427 or 100 μm glass beads or autologous blood clots.^{8,18,22,26,32}
 428 However, in species with higher pulmonary vascular reactivity
 429 such as pigs and goats, Z_C increased.^{18,32} Others have
 430 suggested that this species-dependent lack of change in Z_C
 431 indicates that any increase in Z_C by embolization-induced
 432 pulmonary hypertension is compensated by passive vessel
 433 distension, the capacity for which is species dependent.
 434 ^{3,18,32} Characteristic impedance is also calculated over
 435 varying frequency ranges: 2–12 Hz², above 2 Hz²³ and
 436 above the frequency of the first minimum.¹⁹ We chose to
 437 calculate Z_C by using the frequencies above the first mini-
 438 mum,²⁵ which was approximately 5 Hz at baseline.

439 More insight into the changes in the pulmonary vascula-
 440 ture with embolization can be gained from an in-depth anal-
 441 ysis of the frequency-dependent changes in the pulmonary
 442 vascular impedance spectrum, such as is being pursued for
 443 clinical application.¹⁴ In particular, f_{\min} and R_w are related
 444 to the major reflecting sites in the pulmonary vascular net-
 445 work.²⁰ In this study, f_{\min} increased with embolization, from
 446 5 Hz to at least 20 Hz. In the healthy lungs of dogs, minipigs,
 447 and humans, f_{\min} is in the 2–4 Hz range^{18,20} whereas
 448 after embolization in dogs and minipigs, f_{\min} shifts to 5–
 449 12 Hz.^{7,8,18,22} This increase in f_{\min} with embolization is due
 450 to a more proximal location of the major reflecting sites in
 451 the pulmonary arteries.⁷ The increase in calculated index
 452 of wave reflection with embolization, which also has been
 453 shown to occur in larger animal models,^{8,18} is consistent
 454 with a more proximal location of the major reflecting sites.
 455 In healthy animals, f_{\min} varies due to differences in the
 456 location of wave reflection sites as a function of animal size
 457 and vascular anatomy, and tends to be higher for smaller
 458 animals.²⁰

459 The shift in the location of major reflecting sites should
 460 be a function of the size and distribution of emboli. To fur-
 461 ther explore this issue, we investigated the distribution of
 462 emboli by quantifying the percent obstructed area of vessels
 463 in the histological sections obtained as described above. In
 464 particular, for each lung cross-section, fields of view were
 465 inspected for vessels containing microspheres. A random
 466 sample of at least 14 vessels containing microspheres was
 467 chosen for quantification. The area of the lumen was mea-
 468 sured with quantitative image analysis tools (MetaVue), and
 469 the obstructed area was measured with color thresholding
 470 for the microspheres. The percent obstructed area was cal-
 471 culated as the ratio of obstructed area to total luminal area
 472 ($\times 100$). The average diameter was calculated as the average
 473 lumen height and width measured with line tools. Vessels
 474 with aspect ratios greater than 2 were excluded. The percent
 475 obstructed area decreased rapidly with increasing average
 476 vessel diameter (Fig. 8). The considerable obstruction by
 477 the microsphere emboli in vessels less than 100 μm in diam-
 478 eter clearly represents new reflection sites after emboliza-
 479 tion, which are more proximally located than the capillary
 480 bed. These new sites are likely responsible for increased

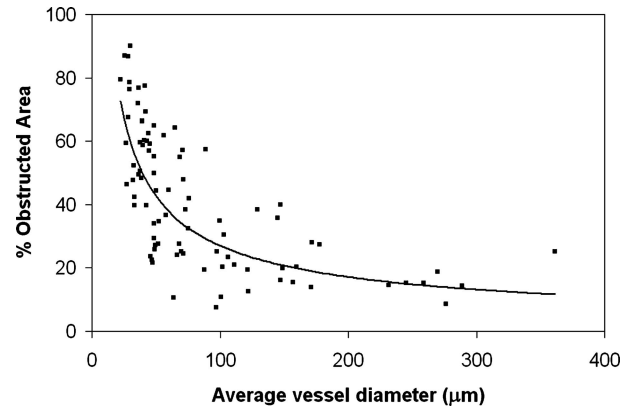


FIGURE 8. Percent obstructed area versus average vessel diameter (D) after second embolization as measured from histological sections from all six animals. Best fit power function trendline shown.

Z values at low frequencies. We might speculate that if all
 the microspheres had completely blocked vessels of 50 μm
 diameter, there would have been a sharp peak in impedance
 at one frequency between 2 and 15 Hz. However, since
 there was a continuous distribution of size of vessels that
 were blocked, there was also a continuous distribution of
 reflection sites after embolization and a gradual decrease in
 Z with frequency between 2 and 15 Hz.

Experimental Considerations

Vascular smooth muscle contraction as a function of
 pressure, flow rate, or embolization was not assessed in this
 study and cannot be discounted because of the availability
 of calcium (100 mg/L calcium nitrate tetrahydrate) in the
 RPMI media. Contraction of smooth muscle cells could
 have been eliminated by using a calcium-free solution as
 a perfusate or by using a vasodilator such as papaverine.
 Alternatively, the impact of smooth muscle cell contraction
 could have been assessed by adding vasoconstrictors such
 as norepinephrine or serotonin to the perfusate. However,
 our goal was to determine the effects of emboli on P_{PA} ,
 PVR, and the impedance spectrum in the presence of normal
 vascular tone.

In all isolated lung systems, the measured pressures de-
 pend on the choice of perfusate, in particular its viscosi-
 ty. The 3.5% Ficoll in RPMI perfusate was chosen based
 on previous isolated lung studies^{10,31,33} and as mentioned
 above, the pressures obtained here were comparable at the
 same flow rates. The viscosity of the Ficoll-RPMI perfusate
 was approximately 3-fold lower than blood: 1.1 cP com-
 pared to about 3.5 cP commonly reported for blood. Dextran
 was used to increase viscosity in preliminary experiments,
 but there was a high prevalence of edema in the lungs with
 this perfusate.

514 Subphysiological flow rates also were used to prevent
 515 edema. The isolated, perfused mouse lung system was
 516 developed for steady flow perfusion, and has most often
 517 been used at very low flow rates (≤ 1 ml/min).^{1,27,31} A
 518 recent study of hypoxic pulmonary vasoconstriction with
 519 various perfusates in an isolated lung system used both
 520 1 ml/min and 3 ml/min steady flow rates without reported
 521 edema.³³ The flow rates used in this study (1–5 ml/min)
 522 were experimentally determined to cover as much of the
 523 physiologic range as possible without compromising lung
 524 function. In preliminary experiments, higher flow rates,
 525 especially under steady flow conditions, generally caused
 526 rapid and irreversible edema.

527 In this isolated lung study, measurements were taken
 528 when lungs were inflated to an end-inspiratory airway pres-
 529 sure $P_{\text{air}} = 10$ cmH₂O, or ~ 7.4 mmHg. We used end-
 530 inspiratory instead of end-expiratory pressure because in
 531 preliminary experiments (without Ficoll), taking measure-
 532 ments at lower pressures occasionally led to irreversible
 533 edema. For steady flow perfusion greater than 3 ml/min,
 534 P_{LA} was greater than P_{air} and thus the lungs were in zone
 535 3 conditions at baseline and after each embolization. How-
 536 ever, for steady flow perfusion at 3 ml/min or less, zone 1
 537 conditions likely occurred. As mentioned above, the shift
 538 from zone 1 to zone 3 conditions may have affected the
 539 $\Delta P - Q$ relationships found here. Also, zone 1 conditions
 540 may have occurred during pulsatile perfusion especially
 541 at transiently low flow rates. Nevertheless, since the cap-
 542 illaries are distal to the emboli and the pressure changes
 543 caused by the emboli, the capillary perfusion pressures
 544 should be comparable at baseline and after embolization.
 545 Thus, the shifts from zone 1 to 2 to 3 conditions should
 546 occur at comparable flow rates, and the significance differ-
 547 ences between baseline and embolization found here should
 548 hold.

549 CONCLUSIONS

550 In this study, we demonstrated that pulsatile flow can be
 551 used in an isolated, ventilated, and perfused mouse lung to
 552 characterize the pulsatile pressure-flow rate relationships
 553 in the mouse pulmonary vascular network. Our results
 554 demonstrate that pulmonary artery pressure, resistance, and
 555 impedance increased with pulmonary embolization in ways
 556 consistent with *in vivo* studies in larger animals and humans.
 557 In particular, the pressure drop across the pulmonary vas-
 558 cular network and PVR increased after embolization, and
 559 frequency-dependent features of the pulmonary vascular
 560 impedance spectrum were suggestive of shifts in the loca-
 561 tions of the major pulmonary vascular reflection sites with
 562 embolization. The flow- and frequency-dependent changes
 563 we found demonstrate the usefulness of the isolated, venti-
 564 lated, and perfused mouse lung for investigations into both
 565 steady and pulsatile pressure-flow rate relationships in the
 566 mouse.

ACKNOWLEDGMENTS

567

This research was supported by the Whitaker Foun- 568
 dation (Biomedical Engineering Research Grant RG-02- 569
 0618). The authors would like to thank Nidal E. Muvarak 570
 for his excellent tissue preservation and histology work and 571
 Rebecca Vanderpool for additional technical assistance. 572

REFERENCES

573

- ¹Archer, S. L., H. L. Reeve, E. Michelakis, L. Puttagunta, R. 574
 Waite, D. P. Nelson, M. C. Dinauer, and E. K. Weir. O₂ sensing 575
 is preserved in mice lacking the gp91 phox subunit of nadh 576
 oxidase. *Proc. Natl. Acad. Sci. USA* 96:7944–7949, 1999. 577
- ²Bergel, D. H., and W. R. Milnor. Pulmonary vascular impedance 578
 in the dog. *Circ. Res.* 16:401–415, 1965. 579
- ³Calvin, J. E. Jr., R. W. Baer, and S. A. Glantz. Pulmonary artery 580
 constriction produces a greater right ventricular dynamic after- 581
 load than lung microvascular injury in the open chest dog. *Circ.* 582
Res. 56:40–56, 1985. 583
- ⁴Caro, C. G., and D. A. McDonald. The relation of pulsatile 584
 pressure and flow in the pulmonary vascular bed. *J. Physiol.* 585
 157:426–453, 1961. 586
- ⁵Ehrhart, I. C., W. M. Granger, and W. F. Hofman. Effects of 587
 arterial pressure on lung capillary pressure and edema after mi- 588
 croembolism. *J. Appl. Physiol.* 60:133–140, 1986. 589
- ⁶Ehrhart, I. C., and W. F. Hofman. Segmental vascular pressures 590
 in lung embolism. *J. Appl. Physiol.* 74:2502–2508, 1993. 591
- ⁷Elkins, R. C., M. D. Peyton, and L. J. Greenfield. Pulmonary 592
 vascular impedance in chronic pulmonary hypertension. *Surgery* 593
 76:57–64, 1974. 594
- ⁸Ewalenko, P., S. Brimiouille, M. Delcroix, P. Lejeune, and R. 595
 Naeije. Comparison of the effects of isoflurane with those of 596
 propofol on pulmonary vascular impedance in experimental 597
 embolic pulmonary hypertension. *Br. J. Anaesth.* 79:625–630, 598
 1997. 599
- ⁹Fagan, K. A., M. Oka, N. R. Bauer, S. A. Gebb, D. D. Ivy, K. G. 600
 Morris, and I. F. McMurtry. Attenuation of acute hypoxic pul- 601
 monary vasoconstriction and hypoxic pulmonary hypertension 602
 in mice by inhibition of rho-kinase. *Am. J. Physiol. Lung Cell* 603
Mol. Physiol. 287:L656–664, 2004. 604
- ¹⁰Fagan, K. A., R. C. Tyler, K. Sato, B. W. Fouty, K. G. Morris 605
 Jr., P. L. Huang, I. F. McMurtry, and D. M. Rodman. Relative 606
 contributions of endothelial, inducible, and neuronal nos to tone 607
 in the murine pulmonary circulation. *Am. J. Physiol.* 277:L472– 608
 478, 1999. 609
- ¹¹Glenny, R. W., S. L. Bernard, and W. J. Lamm. Hemodynamic ef- 610
 fects of 15-microm-diameter microspheres on the rat pulmonary 611
 circulation. *J. Appl. Physiol.* 89:499–504, 2000. 612
- ¹²Hasegawa, J., K. F. Wagner, D. Karp, D. Li, J. Shibata, M. 613
 Heringlake, L. Bahlmann, R. Depping, J. Fandrey, P. Schmucker, 614
 and S. Uhlig. Altered pulmonary vascular reactivity in mice 615
 with excessive erythrocytosis. *Am. J. Respir. Crit. Care Med.* 616
 169:829–835, 2004. 617
- ¹³Hasinoff, I., J. Ducas, U. Schick, and R. M. Prewitt. Pulmonary 618
 vascular pressure-flow characteristics in canine pulmonary em- 619
 bolism. *J. Appl. Physiol.* 68:462–467, 1990. 620
- ¹⁴Huez, S., S. Brimiouille, R. Naeije, and J. L. Vachiery. Feasi- 621
 bility of routine pulmonary arterial impedance measurements in 622
 pulmonary hypertension. *Chest* 125:2121–2128, 2004. 623
- ¹⁵Kafi, S. A., C. Melot, J. L. Vachiery, S. Brimiouille, and R. 624
 Naeije. Partitioning of pulmonary vascular resistance in primary 625

- 626 pulmonary hypertension. *J. Am. Coll. Cardiol.* 31:1372–1376,
627 1998.
- 628 ¹⁶Kussmaul, W. G., A. Noordergraaf, and W. K. Laskey. Right
629 ventricular-pulmonary arterial interactions. *Ann. Biomed. Eng.*
630 20:63–80, 1992.
- 631 ¹⁷Littler, C. M., K. G. Morris Jr., K. A. Fagan, I. F. McMurtry,
632 R. O. Messing, and E. C. Dempsey. Protein kinase c-epsilon-
633 null mice have decreased hypoxic pulmonary vasoconstriction.
634 *Am. J. Physiol. Heart Circ. Physiol.* 284:H1321–1331,
635 2003.
- 636 ¹⁸Maggiolini, M., S. Brimiouille, D. De Canniere, M. Delcroix,
637 and R. Naeije. Effects of pulmonary embolism on pulmonary
638 vascular impedance in dogs and minipigs. *J. Appl. Physiol.*
639 84:815–821, 1998.
- 640 ¹⁹McDonald, D. A. *Blood Flow in Arteries*. London: Edward
641 Arnold, 1974.
- 642 ²⁰Milnor, W. R., *Hemodynamics*. Baltimore, MD: Williams &
643 Wilkins, 1989.
- 644 ²¹Naeije, R. Pulmonary vascular resistance. A meaningless variable.
645 *Intensive Care Med.* 29:526–529, 2003.
- 646 ²²Naeije, R., J. M. Maarek, and H. K. Chang. Pulmonary vascular
647 impedance in microembolic pulmonary hypertension: Effects
648 of synchronous high-frequency jet ventilation. *Respir. Physiol.*
649 79:205–217, 1990.
- 650 ²³Nichols, W. W., C. R. Conti, W. E. Walker, and W. R. Milnor.
651 Input impedance of the systemic circulation in man. *Circ. Res.*
652 40:451–458, 1977.
- 653 ²⁴Nichols, W. W., and M. F. O'Rourke. *McDonald's Blood Flow
654 in Arteries: Theoretical, Experimental, and Clinical Principles*.
655 New York: Oxford University Press, 2005.
- 656 ²⁵Nichols, W. W., M. F. O'Rourke, C. Hartley, and D. A.
657 McDonald. *McDonald's blood flow in arteries: Theoretical,
658 experimental, and clinical principles*. New York: Oxford Uni-
659 versity Press, 1998.
- ²⁶Pagnamenta, A., P. Fesler, A. Vandinivit, S. Brimiouille,
and R. Naeije. Pulmonary vascular effects of
dobutamine in experimental pulmonary hypertension. *Crit.
Care Med.* 31:1140–1146, 2003.
- ²⁷Parker, J. C., M. N. Gillespie, A. E. Taylor, and S. L. Martin.
Capillary filtration coefficient, vascular resistance, and compli-
ance in isolated mouse lungs. *J. Appl. Physiol.* 87:1421–1427,
1999.
- ²⁸Reeves, J. T., J. H. Linehan, and K. R. Stenmark. Distensibility
of the normal human lung circulation during exercise. *Am. J.
Physiol. Lung Cell Mol. Physiol.* 288:L419–425, 2005.
- ²⁹Riegger, G. A., and P. Hoferer. A new experimental model
for measurement of pulmonary arterial haemodynamic vari-
ables in conscious rats before and after pulmonary embolism
and during general anaesthesia. *Cardiovasc. Res.* 24:340–344,
1990.
- ³⁰Taylor, A. E. *Clinical Respiratory Physiology*. Philadelphia, PA:
Saunders, 1989.
- ³¹von Bethmann, A. N., F. Brasch, R. Nusing, K. Vogt, H. D.
Volk, K. M. Muller, A. Wendel, and S. Uhlig. Hyperventilation
induces release of cytokines from perfused mouse lung. *Am. J.
Respir. Crit. Care Med.* 157:263–272, 1998.
- ³²Wauthy, P., A. Pagnamenta, F. Vassalli, R. Naeije, and S.
Brimiouille. Right ventricular adaptation to pulmonary hyperten-
sion: An interspecies comparison. *Am. J. Physiol. Heart Circ.
Physiol.* 286:H1441–1447, 2004.
- ³³Weissmann, N., E. Akkayagil, K. Quanz, R. T. Schermuly,
H. A. Ghofrani, L. Fink, J. Hanze, F. Rose, W. Seeger, and F.
Griminger. Basic features of hypoxic pulmonary vasoconstriction
in mice. *Respir. Physiol. Neurobiol.* 139:191–202, 2004.
- ³⁴Zhao, L., N. A. Mason, N. W. Morrell, B. Kojonazarov, A.
Sadykov, A. Maripov, M. M. Mirrakhimov, A. Aldashev, and
M. R. Wilkins. Sildenafil inhibits hypoxia-induced pulmonary
hypertension. *Circulation* 104:424–428, 2001.